

Electrochemical lithium insertion into $\text{In}_{16}\text{Sn}_4\text{S}_{32}$ and $\text{Cu}_4\text{In}_{20}\text{S}_{32}$ spinel sulphides

J. Morales^a, J.L. Tirado^{a,*}, M.L. Elidrissi Moubtassim^b, J. Olivier-Fourcade^b,
J.C. Jumas^b

^a *Laboratorio de Química Inorgánica, Facultad de Ciencias, Universidad de Córdoba, ES-14004 Córdoba, Spain*

^b *Laboratoire de Physico-chimie des Matériaux Solides, Université de Montpellier 2, 34095 Montpellier Cedex 5, France*

Received 14 June 1994

Abstract

$\text{Cu}_4\text{In}_{20}\text{S}_{32}$ and $\text{In}_{16}\text{Sn}_4\text{S}_{32}$ spinel compounds are used as cathode material in $\text{Li}/\text{LiClO}_4(\text{PC})/\text{sulphide}$ cells. For both compounds, incremental capacity vs. voltage curves and diffusion coefficients vs. composition curves showed two consecutive steps of intercalation. The first step occurs between $x=0$ and $x=8$ for both compositions and at a higher voltage for the tin compound. For larger x values an extended plateau is observed in the voltage vs. composition curves. Cation redistribution is observed during the first insertion step leading to a displacement of In ions from either 8a or 16d sites to another set of octahedral 16c sites in the $Fd\bar{3}m$ space group. This process is more marked in the copper compound owing to the absence of tetrahedral vacancies in the pristine phase and conditions a lower diffusivity of lithium ions.

Keywords: Electrochemical lithium insertion; Spinel sulphides; Indium; Copper

1. Introduction

A wide range of solids of different lattice dimensionality provide suitable host lattices for insertion reactions. Spinel oxides and chalcogenides of structural formula $(\text{A})[\text{B}_2]\text{X}_4$ ($Fd\bar{3}m$ space group; X represents O, S, Se atoms in 32e sites; A represents metal atoms in 8a sites; B represents metal atoms in 16d sites) are prototypical three-dimensional lattices owing to the presence of a rigid framework of alternate rows of edge-sharing BX_6 octahedra joined to AX_4 tetrahedra by corner sharing. Since the observation by Eisenberg [1] that lithium could be reversibly inserted into copper, nickel and copper, and cobalt thiospinels, extensive studies on the insertion properties of transition metal spinel oxides [2–5] and chalcogenides [6] and rare earth thiospinels and selenospinel [7] have been reported. A common behaviour has been found in solids with AB_2X_4 stoichiometry, which was first described by Thackeray et al. [2]: the $[\text{B}_2]\text{X}_4$ framework remains unaltered on lithium insertion, while the A metal ions are displaced to an extra set of octahedral sites (16c sites of the $Fd\bar{3}m$ space group) because of the elec-

trostatic repulsion between A cations and the lithium ions inserted in 16c sites.

A different insertion behaviour has been observed in cation-deficient thiospinels [7–9] with $(\text{A}_y)[\text{B}_2]\text{X}_4$ ($1 > y > 0$) stoichiometry. Topotactic lithium insertion at the 16c sites was observed when the number of A site cation vacancies inhibited the spinel to rock salt first-order transition. A higher lithium ion mobility has also been reported in these defect spinels, owing to larger bottlenecks between 8a tetrahedra and 16d octahedra than in spinel compounds with filled 8a sites. Thus, the cycling performance of lithium cells that use these materials as a cathode is increased [9].

Solid solution indium thiospinels include compounds with AB_2S_4 stoichiometry, as well as cation-deficient solids. A well-documented example of the former stoichiometry is $\text{Cu}_4\text{In}_{20}\text{S}_{32}$. In this compound, partial ordering of copper and indium atoms in tetrahedral sites and off-centre displacement of octahedral cations condition the existence of two sets of tetrahedrally coordinated cations in the 4a and 4c equivalent sites of the $Fd\bar{3}m$ space group [10]. On the contrary, the defect spinel In_2S_3 , with extended formula $(\text{In}_{5.33}\square_{2.66})[\text{In}_{16}]\text{S}_{32}$,

* Corresponding author.

and its solid solutions in the $\text{SnS-In}_2\text{S}_3\text{-SnS}_2$ pseudoternary system are typical examples of cation-deficient spinel compounds with cation vacancies in 8a sites of the $Fd\bar{3}m$ space group [11]. Lithium insertion into the cation-deficient spinel sulphide $(\text{In}_4\text{□}_4)[\text{In}_{12}\text{Sn}_4]\text{S}_{32}$ was studied recently by ^{119}Sn Mössbauer and ^7Li nuclear magnetic resonance spectroscopy [12,13]. Sn^{IV} reduction with insertion and the presence of Li ions in two different sites of the spinel network were observed.

Here we consider the electrochemical behaviour of lithium batteries using $\text{Cu}_4\text{In}_{20}\text{S}_{32}$ and $\text{In}_{16}\text{Sn}_4\text{S}_{32}$ spinels as cathode material. A comparison of thermodynamic, kinetic and structural data is carried out in order to give new light on the effect of cation vacancies on lithium insertion into post transition metal thiospinels.

2. Experimental details

Powdered samples of $\text{Cu}_4\text{In}_{20}\text{S}_{32}$ and $\text{In}_{16}\text{Sn}_4\text{S}_{32}$ thiospinels were prepared as described elsewhere [11,14]. The electrochemical measurements were carried out in $\text{Li/LiClO}_4(\text{PC})/\text{thiospinel}$ cells prepared inside the drybox (M. Braun) by placing a clean lithium metal disk, two glass fibre separators soaked with the electrolyte solution and a pellet of the sulphide concerned into a Teflon container with two stainless steel terminals. The cathode pellets (7 mm diameter) were prepared by pressing 20–30 mg of pure compound. Galvanostatic intermittent titration technique (GITT) and step potential electrochemical spectroscopy (SPES) were carried out at 25 °C by using a multichannel microprocessor-controlled system (MacPile). An initial relaxation of the cells was allowed until the condition $\Delta V/\Delta t \leq 1 \text{ mV h}^{-1}$ was attained. For GITT, voltage relaxation was measured until $\Delta V/\Delta t \leq 1 \text{ mV h}^{-1}$, after -0.04 mA steps of 4 h duration. The SPES spectra were recorded with -10 mV h^{-1} voltage steps. The average lithium content of the cathode material was calculated from the amount of electron charge transferred to the active material, on the assumption that no current flow was due to side reactions. X-ray powder diffraction (XPD) was carried out using a Siemens D500 diffractometer furnished with $\text{Cu K}\alpha$ radiation and a graphite monochromator. For intercalated phases, a plastic fibre was used to cover the sample in order to avoid undesirable reactions with air during the recording. Rietveld refinements were carried out with the aid of the computer program DBWS-9006 [15].

3. Results and discussion

Typical GITT curves obtained in the composition interval $14 \geq x \geq 0$ are shown in Fig. 1 for $\text{Li}_x\text{In}_{16}\text{Sn}_4\text{S}_{32}$ and $\text{Li}_x\text{Cu}_4\text{In}_{20}\text{S}_{32}$. The open-circuit voltage vs. x curve

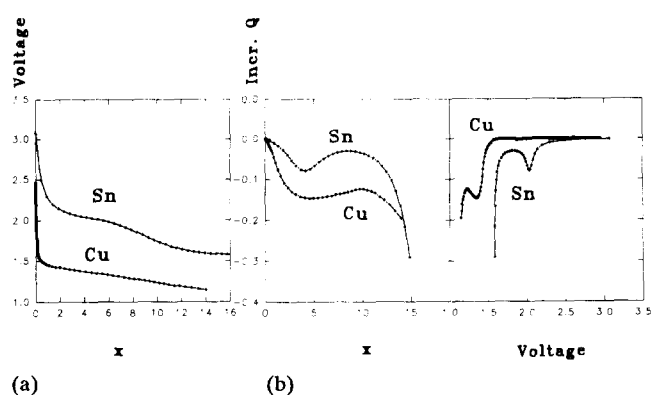


Fig. 1. (a) Galvanostatic titration curves of $\text{Li/LiClO}_4(\text{PC})/\text{thiospinel}$ cells. (b) Plots of incremental capacity vs. composition and cell voltage.

consisted of an initial abrupt decrease in voltage followed by two consecutive plateaux. The initial decrease in voltage is more marked for the copper compound, while the two steps are more clearly resolved for tin thiospinel. From these results, it can be derived that lithium intercalation into $\text{Li}_x\text{In}_{16}\text{Sn}_4\text{S}_{32}$ is thermodynamically more favourable than into $\text{Li}_x\text{Cu}_4\text{In}_{20}\text{S}_{32}$, as the free energy of intercalation is simply the Faraday constant multiplied by the area below the titration curve [16]. For both compounds, incremental capacity vs. voltage curves showed a first minimum followed by an extended effect. The first peak is located at ca. 2 V for the tin and at ca. 1.4 V for the copper compound. Irrespective of this difference in voltage, the plot of incremental capacity vs. x evidences that the first effect takes place between $x=3$ and $x=9$ for both compositions.

The lithium ion diffusion coefficients were alternatively obtained from potentiostatic and GITT measurements. For SPES measurements the method described in Ref. [17] was used. Fig. 2 shows a typical kinetic plot for copper thiospinel, from which the slopes of the plots of the logarithm of the intensity vs. time for long relaxation times were used to obtain the diffusion coefficient according to

$$d \log |i|/dt = -\pi^2 D/4L^2 \quad (1)$$

where L is the diffusion path, which was assumed to be the thickness of the pellets (ca. 0.3 mm).

For GITT measurements, the Honders method [18] was applied and the diffusion coefficients were evaluated from the evolution of voltage vs. time such as the examples shown in Fig. 2. For long relaxation times, it was observed that the difference $\Delta E'$ between ΔE and the straight line obtained by extrapolating the linear part of the ΔE vs. $t^{1/2}$ plot varies linearly with time. The chemical diffusion coefficient can then be evaluated by the expression

$$D = (4/\pi)[L(d \Delta E'/dt)/(d \Delta E/dt^{1/2})]^2 \quad (2)$$

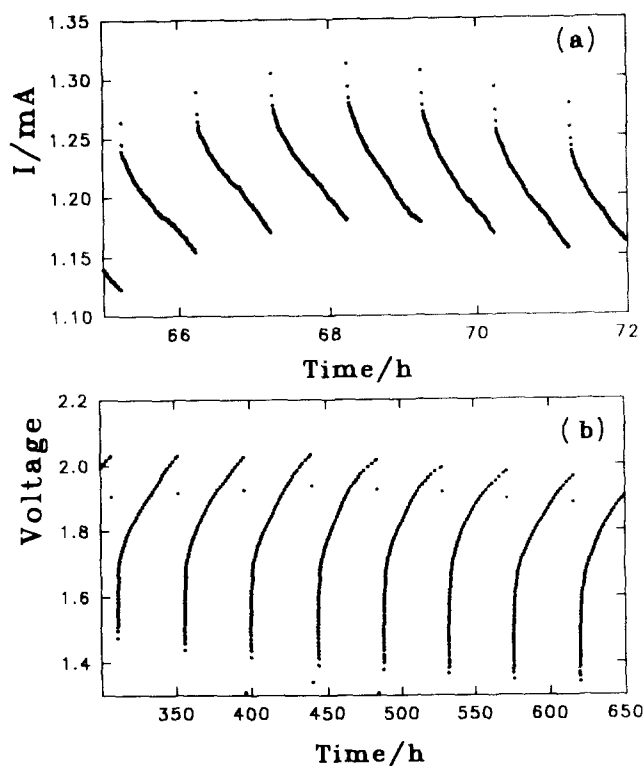


Fig. 2. Kinetic plots obtained by (a) SPES of $\text{Li}_x\text{Cu}_4\text{In}_{20}\text{S}_{32}$ and (b) GITT of $\text{Li}_x\text{In}_{16}\text{Sn}_4\text{S}_{32}$.

The measured D values took values in the 10^{-6} – 10^{-7} $\text{cm}^2 \text{s}^{-1}$ interval for tin and in the 10^{-8} – 10^{-9} $\text{cm}^2 \text{s}^{-1}$ interval for copper. These values are comparable with those found in two-dimensional chalcogenide systems, such as TiS_2 [19]. When plotted vs. depth of discharge (Fig. 3) the diffusion coefficients reveal a gradual increase up to 4 F mol^{-1} followed by a decrease that reaches a minimum close to 8 F mol^{-1} for both compositions. A new increasing trend occurs for $x > 9$ that reaches values below 10^{-7} $\text{cm}^2 \text{s}^{-1}$.

The electrochemical results can be interpreted in terms of two different intercalation phenomena. In the light of previous work on chemical insertion into this system and the stoichiometry and cation vacancies in the structure of this solid, the first zone of the discharge can be ascribed to $\text{Sn}^{\text{IV}}/\text{Sn}^{\text{II}}$ and $\text{In}^{\text{III}}/\text{In}^{\text{I}}$ reduction which is accompanied by Li insertion into a similar set of equivalent sites in the structure, mainly octahedrally coordinated 16c sites of the $Fd\bar{3}m$ space group, which are particularly favourable for the diffusion of lithium ions. Further insertion results in In^{III} reduction and probable lithium occupancy of tetrahedrally coordinated sites 8a and 48f.

Powder X-ray diffraction data provide additional evidence of this complex behaviour. The unit cell parameter of the pristine compounds increased slightly after discharge (Table 1), a consequence of lithium insertion in rigid three-dimensional host lattices usually observed [1–9]. In addition, significant changes in the

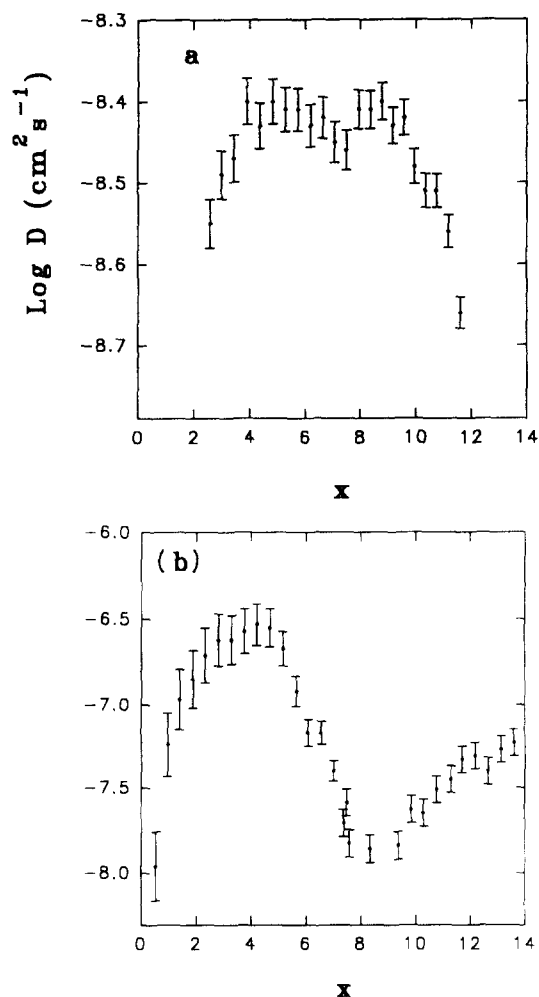


Fig. 3. Compositional variation in the chemical diffusion coefficient of Li^+ intercalated into (a) $\text{Li}_x\text{Cu}_4\text{In}_{20}\text{S}_{32}$ and (b) $\text{Li}_x\text{In}_{16}\text{Sn}_4\text{S}_{32}$.

Table 1

Results of the Rietveld analysis of X-ray diffraction data of tin indium spinel and lithiated products

Composition	a (Å)	m	n	X (32e)	R_{wp}	R_p	R_{exp}
$\text{In}_{16}\text{Sn}_4\text{S}_{32}$	10.7551	4.40	–	0.257	16.4	12.8	9.4
$\text{Li}_2\text{In}_{16}\text{Sn}_4\text{S}_{32}$	10.7665	4.18	2.23	0.258	15.7	12.9	7.9
$\text{Li}_4\text{In}_{16}\text{Sn}_4\text{S}_{32}$	10.7686	4.06	2.27	0.256	16.7	13.8	8.0
$\text{Li}_6\text{In}_{16}\text{Sn}_4\text{S}_{32}$	10.7890	3.60	2.66	0.253	15.8	12.9	8.1
$\text{Li}_8\text{In}_{16}\text{Sn}_4\text{S}_{32}$	10.7783	3.66	3.00	0.255	15.6	12.8	8.3

$(\text{In}_m\text{Sn}_{8-m})_{8a}(\text{In}_x\text{Li}_{16-n-x})_{16c}[\text{In}_{16-m-n}\text{Sn}_4\text{S}_{32}]_{16d}$; $Fd\bar{3}m$, origin at centre $\bar{3}m$, at 1/8, 1/8, 1/8 from $4\bar{3}m$.

intensities of the reflections were observed leading to a particularly enhanced intensity of the 400 line. Such changes have also been detected in lithium-inserted spinel oxides and have been interpreted in terms of the diffusion of strongly scattering cations from tetrahedral to octahedral sites [5–7].

Rietveld refinement of powder X-ray diffraction data was carried out in pristine and intercalated solids (Fig.

4). Although this procedure does not allow a precise determination of the atomic positions of low scattering atoms, such as lithium atoms, it has proven to be of particular interest in the determination of cation distribution in lithium-containing mixed oxides. A structural model based on the following distribution was used to refine site occupancies and coordinates:

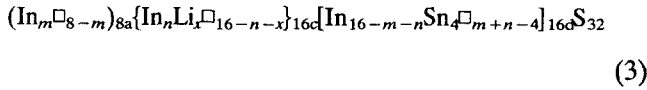


Table 1 shows the results of the Rietveld refinement, in which little changes in the atomic coordinates of sulphur atoms are detected for the different compositions. It should be noted that the initial cation distribution implies that more than half of the tetrahedral 8a sites are occupied by In ions. This occupancy decreases gradually with insertion while In ions are displaced from either 8a or 16d sites to the other set of octahedral 16c sites. Lowering the number of 8a ions decreases electrostatic repulsions with incoming lithium ions and favours lithium diffusion through 16c sites.

This behaviour agrees with the increase in lithium diffusivity during the first steps of insertion, as discussed above. However, a complete displacement of In atoms from 8a sites is not observed, which agrees with the progressive occupancy of 16c sites by lithium ions and the decrease in lithium diffusivity for $x > 4$ as the number of available 16c sites decreases. In fact, for $x = 14$, lithium ions are forced to occupy 8a sites thus leading to a different behaviour, evidenced in the incremental capacity and diffusion coefficients plot. In addition it is noteworthy that cation redistribution also affects the 16d site occupancy by lowering the number of occupied sites in this set, leading to a similar occupancy in 16c and 16d; the extrapolation of this behaviour should lead to the ideal rock salt structure. These observations are consistent with the insertion behaviour found in copper thiospinels, in which cation redistribution is observed even for $Cu_{0.5}MS_4$ compositions [9].

Thus the electrochemical intercalation of lithium into indium tin spinel sulphide can be summarized as follows:

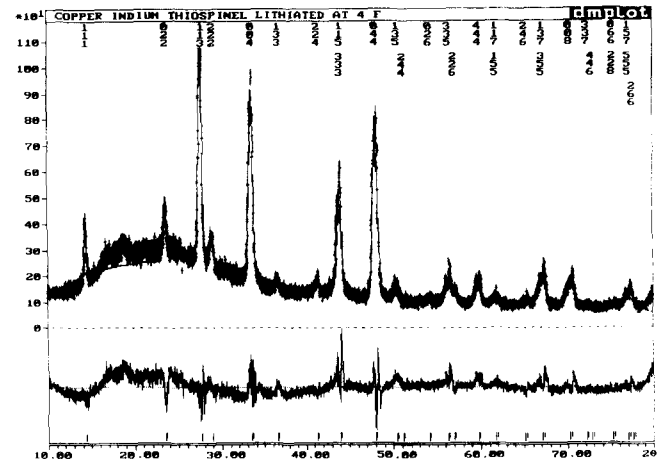
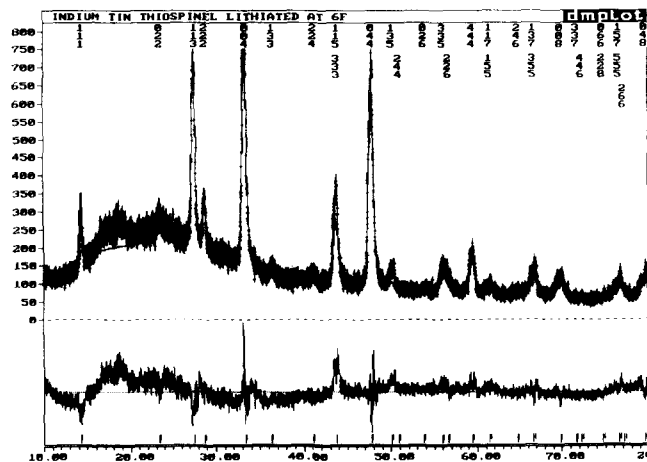
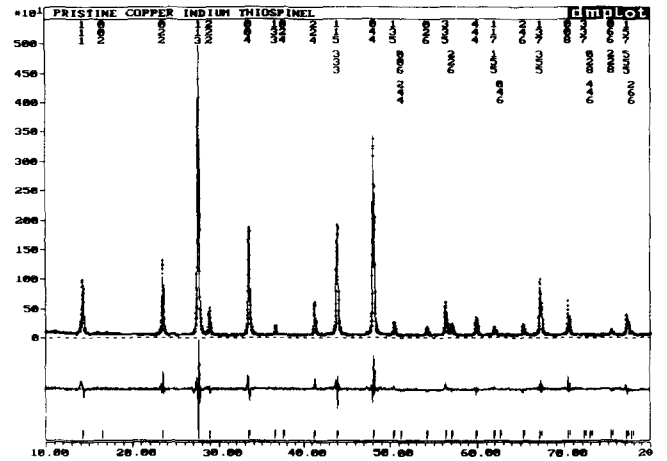
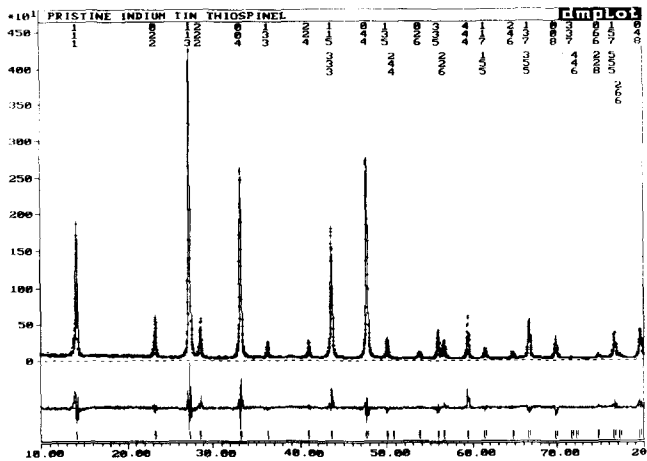


Fig. 4. Selected results of the Rietveld refinement of XPD data.

Table 2
Results of the Rietveld analysis of X-ray diffraction data of copper indium spinel

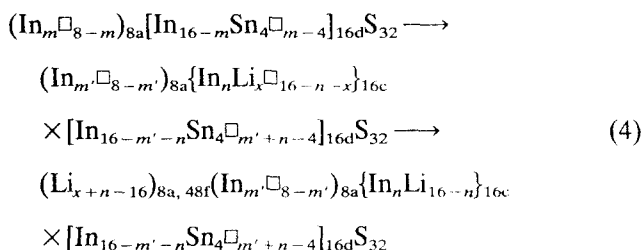
Composition	a (Å)	p	x (16e(1))	x (16e(2))	x (16e(3))	R_{wp}	R_p	R_{exp}
$Cu_4In_{20}S_{32}$	10.6821	2.61	0.621	0.375	0.867	16.4	13.1	9.1

$(Cu_pIn_{4-p})_{4a}(Cu_{4-p}In_p)_{4c}[In_{16}]_{16c(1)}(S_{32})_{16c(2), 16c(3)}$; $F\bar{4}3m$, origin at $\bar{4}3m$.

Table 3
Results of the Rietveld analysis of X-ray diffraction data of lithiated copper indium spinels

Composition	a (Å)	m	n	x (32e)	R_{wp}	R_p	R_{exp}
$Li_xCu_4In_{20}S_{32}$	10.7220	3.27	1.93	0.261	15.2	12.2	7.3
$Li_6Cu_4In_{20}S_{32}$	10.6843	1.99	2.92	0.259	14.5	11.8	7.5

$(In_mCu_4)_{8a}\{In_nLi_{x(16-n-x)}\}_{16c}[In_{20-m-n}Sn_{m+n-4}]_{16d}S_{32}$; $Fd\bar{3}m$, origin at centre $\bar{3}m$, at 1/8, 1/8, 1/8 from $\bar{4}3m$.



For $Cu_4In_{20}S_{32}$, a more complex distribution is expected. Rietveld refinement of the pristine solid in the $F\bar{4}3m$ space group leads to a $(Cu_{2.61}In_{1.39})_{4a}-(Cu_{1.39}In_{2.61})_{4c}[In]_{16c}S_{32}$ cation distribution (Table 2), which is similar to previously reported data on this system. For lithium-inserted solids, however, the existence of two sets of tetrahedrally coordinated sites together with the existence of refinable coordinates for four sets of 16e sites equivalent to 16c, 16d and the two sets of sulphur atoms would lead to a large number of structural parameters that cannot be treated by the Rietveld procedure. However, a better fitting was found by using the $Fd\bar{3}m$ space group as shown in Table 3. The reduction of tetrahedrally coordinated In atoms is more marked than in the tin compound, although the final number of In atoms in 16c sites is similar, as a consequence of the larger metal content of the latter compound. The lower number of metal ions in 8a sites in the tin compound has a lower blocking effect on 16c sites and may explain the larger values of Li^+ ion diffusion coefficients for this composition.

However, the electrochemical insertion of lithium into this system may be of interest towards its application in "Li ion" or "rocking chair" batteries. In fact TiS_2 was recently examined as an anode material vs. $LiCoO_2$

[20]. The observed values of voltage and diffusion coefficients in the $Li/Li_xIn_{16}Sn_4S_{32}$ cell make this system a promising candidate for application in this particular type of advanced batteries.

Acknowledgement

The authors are indebted to the Commission of the European Communities for financial support (Contract JOU2-CT93-0326).

References

- [1] M. Eisenberg, *J. Electrochem. Soc.*, 127 (1980) 2382.
- [2] M.M. Thackeray, W.I.F. David and J.B. Goodenough, *Mater. Res. Bull.*, 17 (1982) 785.
- [3] J.B. Goodenough, M.M. Thackeray, W.I.F. David and P.G. Bruce, *Rev. Chim. Miner.*, 21 (1982) 435.
- [4] C.J. Chen, M. Greenblatt and J.V. Waszczak, *Mater. Res. Bull.*, 21 (1986) 609.
- [5] M. Pernet, P. Strobel, B. Bonnet, P. Bordet and Y. Chabre, *Solid State Ionics*, 66 (1993) 259.
- [6] A.C.W.P. James, B. Ellis and J.B. Goodenough, *Solid State Ionics*, 27 (1988) 45.
- [7] P. de la Mora and J.B. Goodenough, *J. Solid State Chem.*, 70 (1987) 121.
- [8] A.C.W.P. James, J.B. Goodenough and N.J. Clayden, *J. Solid State Chem.*, 77 (1988) 356.
- [9] N. Imanishi, K. Inoue, Y. Takeda and O. Yamamoto, *J. Power Sources*, 43–44 (1993) 619–625.
- [10] L. Gastaldi and L. Scaramuzza, *Acta Crystallogr. B*, 36 (1980) 2751.
- [11] C. Adenis, J. Olivier-Fourcade, J.C. Jumas and E. Philippot, *Rev. Chim. Miner.*, 25 (1987) 10.
- [12] M.L. Elidrissi Moubtassim, J. Olivier Fourcade, J.C. Jumas and J. Senegas, *J. Solid State Chem.*, 87 (1990) 1.
- [13] M.L. Elidrissi Moubtassim, J. Olivier Fourcade, J. Senegas and J.C. Jumas, *Mater. Res. Bull.*, 28 (1993) 1083.
- [14] C. Paorici, L. Zanotti and L. Gastaldi, *Mater. Res. Bull.*, 14 (1979) 469.
- [15] A. Saktivel and R.A. Young, Program DBWS-9006, Georgia Institute of Technology, 1993.
- [16] A.S. Nagelberg and W.L. Worrell, *J. Solid State Chem.*, 29 (1979) 345.
- [17] C.J. Wen, B.A. Boukamp, R.A. Huggins and W. Weppner, *J. Electrochem. Soc.*, 126 (1979) 2258.
- [18] A. Honders, J.M. Der Kinderen, A.H. Van Heeren, J.H.W. Witt and G.H. Broer, *Solid State Ionics*, 15 (1985) 265.
- [19] K. Kanehori, F. Kirino, T. Kudo and K. Miyauchi, *J. Electrochem. Soc.*, 138 (1991) 2216.
- [20] E.J. Plichta and W.K. Behl, *J. Electrochem. Soc.*, 140 (1993) 46.